Analysis (FEA) Software (ANSYS, ABAQUS, MSC Nastran, etc). Hill's yield criterion, which can be considered a generalization of the von Mises criterion, relates yield strength in different directions to a reference yield stress. Creep response can also be described using the Hill model. A detailed description is given in [10-13].

There are no plasticity and creep models of SC material in the popular FEA software. The goal of this study was to develop one. Such models have to be physically-based and readily implementable, but also should not be expensive or time-consuming while obtaining the necessary experimental data.

2. Methods

This paper focused on the following topics:

- Experimental investigation of alloy behavior.
- Plasticity and creep model development and their program implementation.
- Single Crystal blade calculation.

Experimental Studies. In order to study the effect of CO on the characteristics of a SCNBS, a series of tests was carried out at various temperatures for a Russian alloy: tensile test under conditions of short-term and long-term loading. Additionally, torsion tests were conducted at room temperature.

All experiments were carried out for four different COs: [001], [011], [111], [012]. It should be noted that samples with intermediate orientation [012] were tested to check the hypothesis of piecewise linear interpolation of properties, which will be described in more detail later. Fig. 1, 2 show a view of SCNBS specimens.

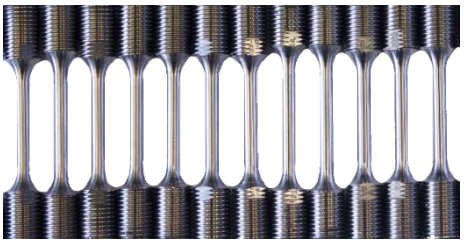

Fig. 1. Specimens for tensile test

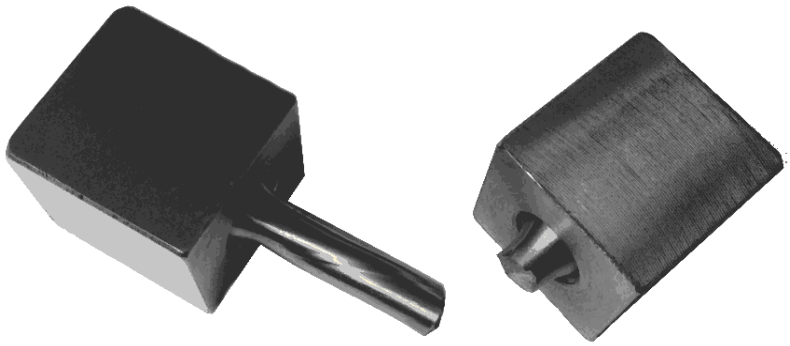

Fig. 2. Specimen after torsion test

Plasticity and Creep Models and Their Program Implementation. SX are characterized by a cubic symmetry of properties, i.e. the crystallographic lattice has three mutually orthogonal planes of symmetry (Fig. 3). One can distinguish three mutually perpendicular directions for which the properties are equal. There are three main families of Crystallographic directions that are vertices of a stereographic triangle: <001>, <011>,

<111> (Fig. 3).

The suggested approach incorporates the cubic symmetry of SX using the generalized Hooke's law:

$$\{\sigma\}=[C]\{\varepsilon\} \text{ or } \{\varepsilon\}=[S]\{\sigma\}, \quad (1)$$

where $\{\sigma\}$, $\{\varepsilon\}$ are tensors of stress and strains and $[C]$, $[S]$ are 4th order tensors of stiffness and compliance.

The elastic properties of SCNBS exhibit cubic symmetry, also described as cubic syngony. The elastic properties of materials with cubic symmetry can be described with three independent constants of the elastic stiffness matrices, C_{11}, C_{12}, ..., C_{44} or the elastic compliances S_{11}, S_{12}, ..., S_{44} (After transition from the tensor notation to the matrix one).

$$[C]=\begin{bmatrix} C_{11} & C_{12} & C_{12} & 0 & 0 & 0 \\ C_{12} & C_{11} & C_{12} & 0 & 0 & 0 \\ C_{12} & C_{12} & C_{11} & 0 & 0 & 0 \\ 0 & 0 & 0 & C_{44} & 0 & 0 \\ 0 & 0 & 0 & 0 & C_{44} & 0 \\ 0 & 0 & 0 & 0 & 0 & C_{44} \end{bmatrix}.$$

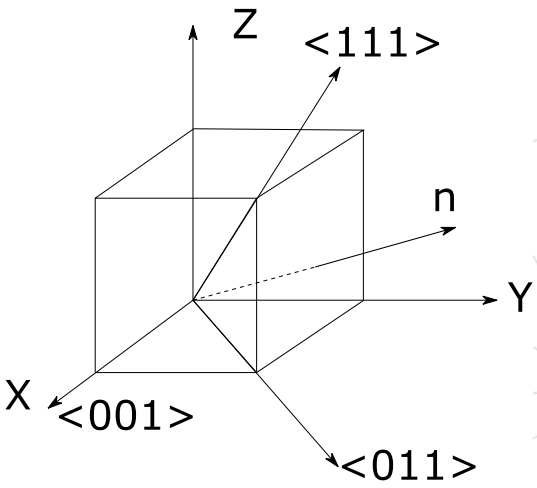

Fig. 3. Single Crystal Axes

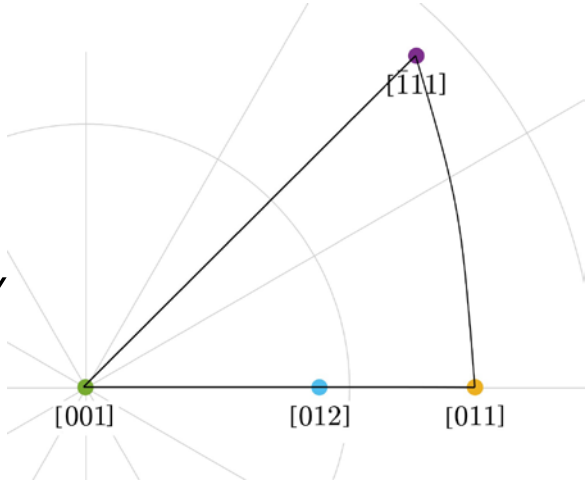

Fig. 4. Stereographic triangle

To determine the elastic modulus in an arbitrary crystallographic direction $\vec{n}$, the dependence is used:

$$E_n=\frac{1}{S_{11}-2\left(S_{11}-S_{12}-\frac{1}{2}S_{44}\right)L}, \quad (2)$$

where L characterizes the direction of $\vec{n}$ with respect to the axes of the SX (Fig. 2) and is equal to zero in the directions <001> and reaches a maximum value of $\frac{1}{3}$ in the <111> direction.

$$L=l_1^2l_2^2+l_2^2l_3^2+l_3^2l_1^2, \quad (3)$$

where, $l_1=\cos\left(\vec{n}\wedge X\right)$, $l_2=\cos\left(\vec{n}\wedge Y\right)$, $l_3=\cos\left(\vec{n}\wedge Z\right)$- direction cosines. This dependence can be shown as a glyph (Fig. 5).

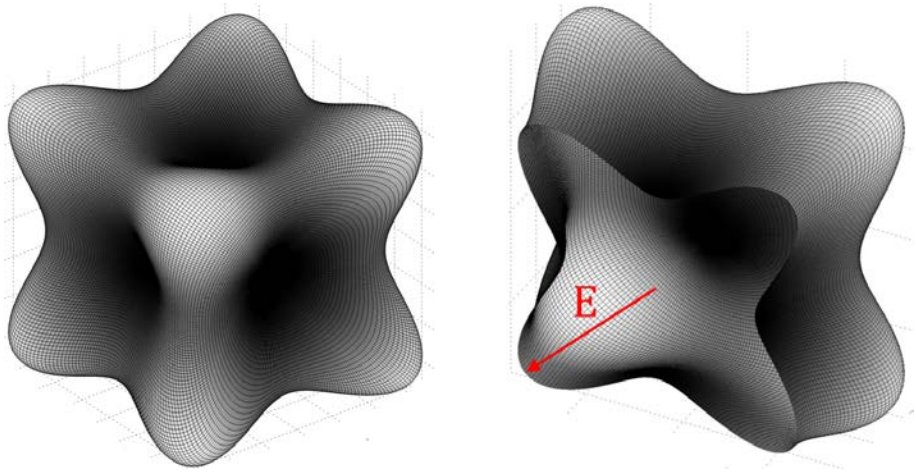

Fig. 5. The glyph represented elastic anisotropy

A yield surface is a map in stress space, in which an inner envelope is drawn to demarcate elastic regions from yielded regions. The yield criterion for polycrystalline material could be written as follows:

$$f = \sigma_e - \sigma_Y(T), \tag{4}$$

where σ_e is the equivalent stress and σ_Y represents the yield strength. A whole range of multiaxial yield criteria exist. The most commonly used criterion in engineering practice, particularly for FE computational analysis, is that of von Mises and Tresca.

For anisotropic materials, the yield surface is much more complicated than for isotropic materials. It is necessary to consider the orientation of the stress state relative to the axes of SX and mechanical properties in different directions. This could be written as follows:

$$F = f(\sigma_1, \sigma_2, \sigma_3, \sigma_Y, \alpha, \beta, \gamma) = 0, \tag{5}$$

where α, β, and γ are the angles characterizing the position of the principal stress axes relative to the main coordinate system. There are number of yield criterion of anisotropic bodies, but their distinctive feature is the complexity of the yield surface (i.e, a function of the equivalent stress).

For the calculations of the elastic-plastic stress-strain state (SSS) by the finite element method for a single-crystal alloy, the authors proposed [1] a plasticity criterion:

$$f = \sigma_e - \sigma_Y(\gamma, T), \tag{6}$$

where γ is the relative orientation between principal stresses and SX axes, T is the temperature, σ_e is equivalent stresses. Stresses by von Mises, Tresca, and unifying them, the Hosford, could be considered as equivalent.

The value of the orientation factor L (3) of the equivalent direction $\vec{T}$ (Fig. 6), determined by (7), is taken in the present study as parameter γ.

$$\vec{T} = \sigma_1 \vec{e_1} + \sigma_2 \vec{e_2} + \sigma_3 \vec{e_3}. \tag{7}$$

Using this value, the yield strength, as well as other mechanical properties (ultimate tensile strength, elongation) defining the deformation curve for the given SSS and temperature (Fig. 7), is calculated for temperature T. The use of piecewise linear dependence is suggested in this study. Elastic modulus is calculated by (2). After determination of the specified parameters, a deformation curve is constructed. It should be noted that tangent modulus is the function of yield strength, ultimate tensile strength, elongation and therefore depends on L.

Many studies have been done on tension/compression asymmetry in the mechanical characteristics of SCNBS [7,14], where authors have shown that this difference can be significant. The suggested approach assigns a sign to equivalent stresses by the sign of mean

normal stress:

$$\sigma_m = \frac{(\sigma_1 + \sigma_2 + \sigma_3)}{3}. \quad (8)$$

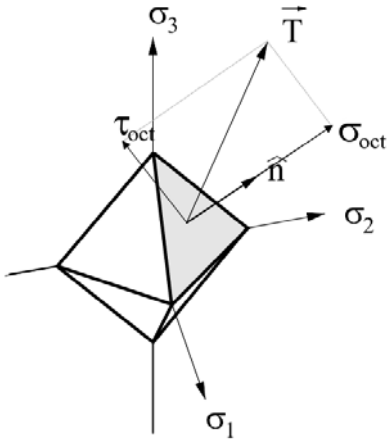

Fig. 6. Equivalent direction

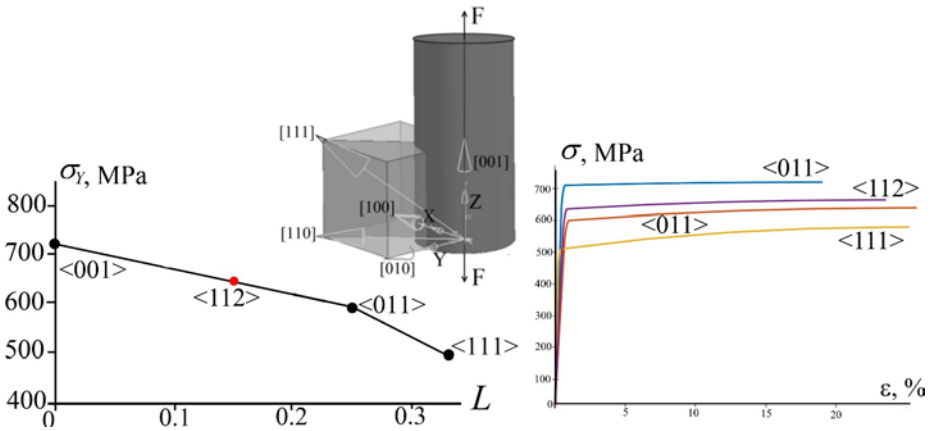

Fig. 7. Yield strength dependence on *L*

In order to consider tension/compression asymmetry, the suggested approach allows us to input asymmetry coefficient as a function of temperature and crystallographic direction. It is an experimentally determined ratio $k_{ac} = \frac{\sigma_Y^{tens}}{\sigma_Y^{compr}}$.

Developed approach allows us to consider the effects of variations of the relative orientation between crystal axes and blades axes on SSS. This approach can be easily reduced to the level of isotropic materials. The computational procedure of SX turbine blade SSS determination using the proposed approach consists of the following steps:

• mechanical FEA produces trial stresses and strains;

• the routine computes the equivalent direction $\vec{T}$ (7) and its orientation factor *L* (3) in every integration point of FEM;

• by the value of *L*, the routine computes material properties defining the deformation curve (yield and ultimate strength, elongation) at every integration point of FEM with its temperature;

• the routine computes the sign of mean normal stress (8);

• in case of a negative value of mean normal stress, the routine adjusts the values of the yield strength (in the case of available data on the characteristics of asymmetry);

• the routine checks the yield criterion (6) for every integration point of FEM;

• the routine constructs the deformation curve $\sigma = f(\varepsilon)$ for integration points where $\sigma_e \geq \sigma_Y$;

• the routine determines the elastic-plastic SSS.

Results of experimental and numerical checking of this approach shown good feasibility [16].

Developed creep subroutine deals with the anisotropy in similar way. By linear interpolation between values for the main CO (<001>, <011>, <111>) routine constructs creep curve for temperature, stress, accumulated state variable, and relative orientation between crystal and blade axes.

Construction of creep curves is carried out using Larson-Miller curves at every integration point with the temperature *T* and stress σ_e.

$$P_{LM} = T(\log_{10} t + C), \tag{9}$$

where *C* – material constant, usually 20; *t* – life, hr.

For isotropic materials, results of this model were compared with experimentally obtained results of High Pressure Turbine (HPT) blade damage and deformation. It was shown that numerical predictions were correct [15].

A feature of this material model is the need to identify the starting point on the creep curve for the calculation of creep. Such an identifier is the accumulated equivalent plastic strain at the stage of elastoplastic calculation. That is, plastic and creep strain are related quantities.

The proposed plasticity and creep models were implemented in the open-source FEA software CalculiX. Modifications were made to the program modules responsible for the physical nonlinearity of the material [16].

Single Crystal blade calculation. The calculations of SSS and static strength on the design mode of the HPT SX model blade with and without anisotropy were carried out for the comparison of strength characteristics. All strength calculations were carried out by three-dimensional finite element method. Operation time on design mode is 100 hours.

Figure 8 shows FEM of the model blade. Figure 9 shows temperature distribution along blade.

The strength calculations of the blade were carried out step by step: at the first stage, the SSS was determined in the elastic-plastic formulation considering the anisotropy of the elastic and plasticity characteristics; at the second, the problem of determining the kinetics of the SSS due to creep (stress relaxation) was solved.

The blade was fixed on the contact edges of the shank. The safety factor value of long-term static strength (K_m) can be determined by the equation:

$$K_m = \frac{\sigma_r\left(T, t, \vec{T}\right)}{\sigma_{eqv}^t}, \tag{10}$$

where σ_r – creep strength, determined for a given temperature, duration and equivalent direction; σ_{eqv}^t – equivalent in time stress. This stress leads to the same damage as constantly changing due to creep stress.

One of the issue when equation (10) is used is to take into account equivalent direction changing due to creep. Below we will compare results for two variants of calculation of safety factor with and without consideration of the changes in *L*. Average integral is being used for such purpose.

It should be noted that Km is connected to the lifetime safety factor according to

formula $K_t = (K_m)^m$, where m – is the parameter characterizing the slope of the long-term static strength curve.

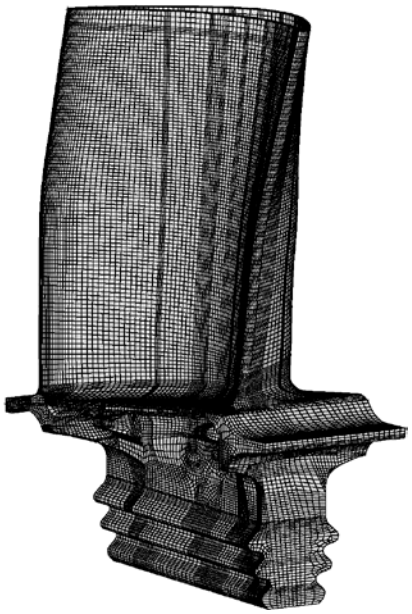

Fig. 8. FE Model

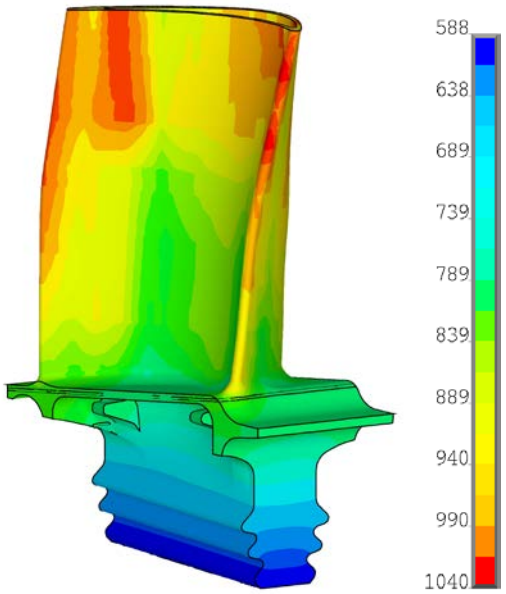

Fig. 9. Temperature distribution, °C

3. Results

Experimental Studies. Torsion and tension experiments of smooth cylindrical specimens of various COs ([001], [011], [111], [012]) were carried out. The deformation curves are presented in Figs. 10, 11. There is a strong anisotropy of the properties of both tensile and torsion during the transition from one CO to another (Table 1).

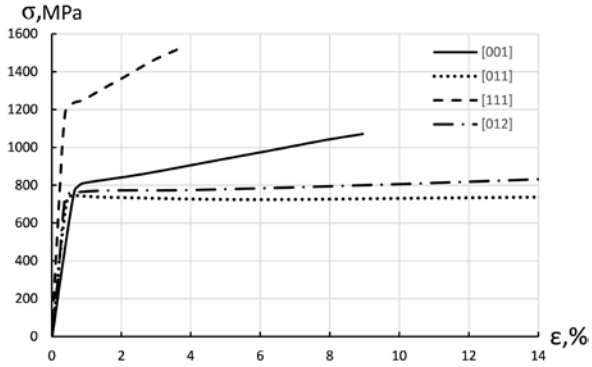

Fig. 10. Deformation Curve at 20ºC

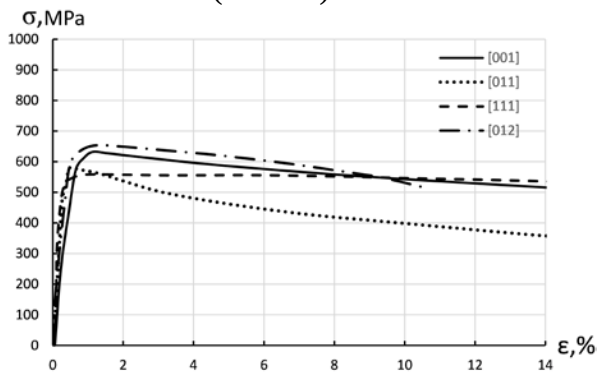

Fig. 11. Deformation Curve at 1000ºC

Table 1. Experimental results

CO	E, GPa	G,GPa
[001]	130	77
[011]	236	41
[111]	325	42
[012]	246	53

Creep strength anisotropy was experimentally investigated for the same SCNBS in this study. The investigation was carried out in a wide range of stresses and temperatures. As expected, creep characteristics are highly dependent on CO. Figure 12 shows some of the results of creep tests. Figure 13 shows Larson-Miller curves.

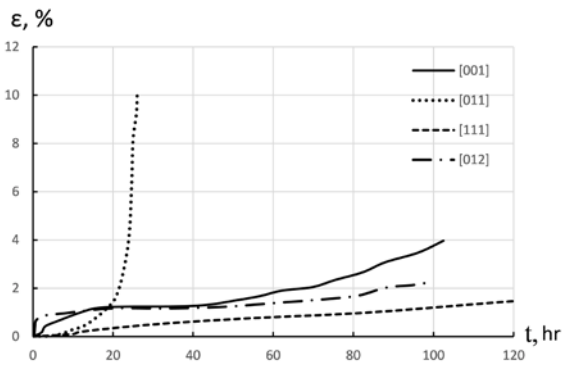

Fig. 12. Creep Curves at T=950ºC, σ=314 MPa

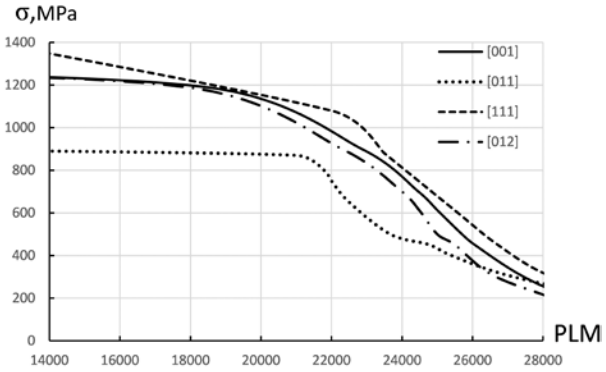

Fig. 13. Larson-Miller curves

Analysis of the results showed that CO [011] is the least favorable in terms of strength characteristics.

Proposed models based on the hypothesis of the possibility of using piecewise linear interpolation of properties in stereographic triangle using orientation factor L. The validity of the accepted hypothesis was tested. Figures 14, 15 show the dependence of yield and unlimate strengths on the orientation factor (3), where the values are 0.0, 0.16, 0.25, 0.33, corresponding to the [001], [012], [011], [111] orientations, respectively.

It is shown that the data for the yield strength and ultimate stress for the intermediate orientation [012] (L = 0.16) are in satisfactory agreement with the hypothesis of linear interpolation of properties between the main CO ([001], [011], [111]), nevertheless it is recommended to obtain material properties in intermediate COs.

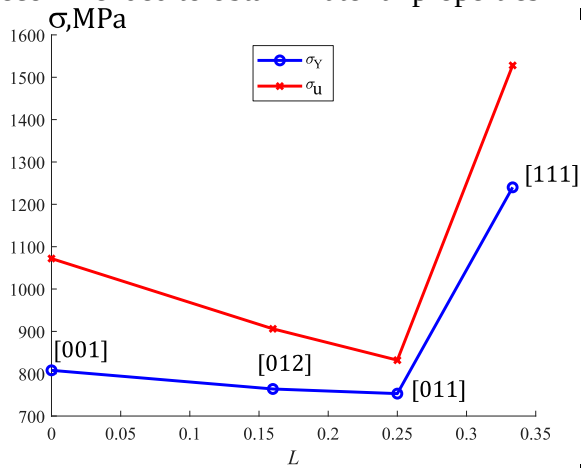

Fig. 14. The value of yield strength dependence on L for 20ºC

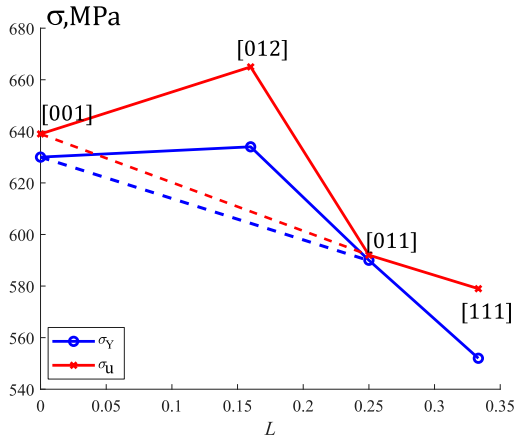

Fig. 15. The value of yield strength dependence on L for 1000ºC

Finite Element Analyses of Turbine Blade. Figures 16, 17 show distribution on the isotropic blade von Mises stress and the local safety factor. "Dangerous" zones with low values of safety factor values are marked by numbers 1,2. First zone is the zone with maximal temperature, second zone is the zone with minimal safety factor value.

After the calculations, the processing of their results was carried out and the magnitudes of changes in the values of stresses and safety factors were found in case of taking into account anisotropy. To do this, we used the following relationship.

$$\Delta\overline{\sigma}_{eqv}^{t} = \frac{\sigma_{eqv}^{iso\_t} - \sigma_{eqv}^{aniso\_t}}{\sigma_{eqv}^{iso\_t}}, \qquad (11)$$

$$\Delta\overline{K}_m = \frac{K_m^{iso} - K_m^{aniso}}{K_m^{iso}}. \quad (12)$$

A negative value means a decrease in magnitude in case of anisotropy consideration.

Figures 18, 19 show distribution on the blade differences of the results. Table 1 shows results for two calculation with and without anisotropy consideration in "dangerous" zones, where σ_0 – von Mises stress at the end of elastoplastic strain; σ_{end} – von Mises stress after 100 hr of working on regime; σ_{eqv}^t – equivalent in time von Mises stress.

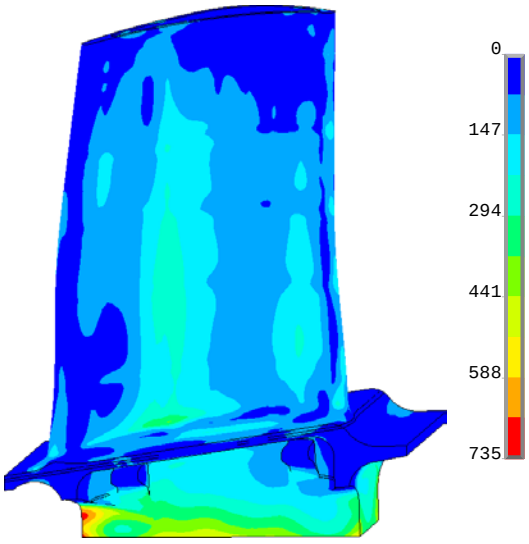

Fig. 16. Distribution of σ_0, MPa

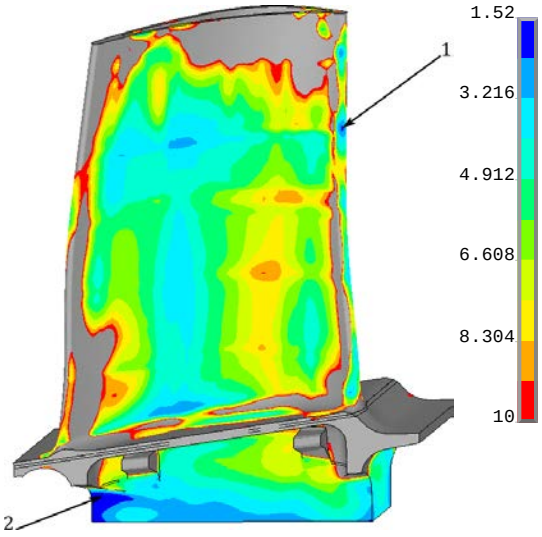

Fig. 17. Distribution of K_m

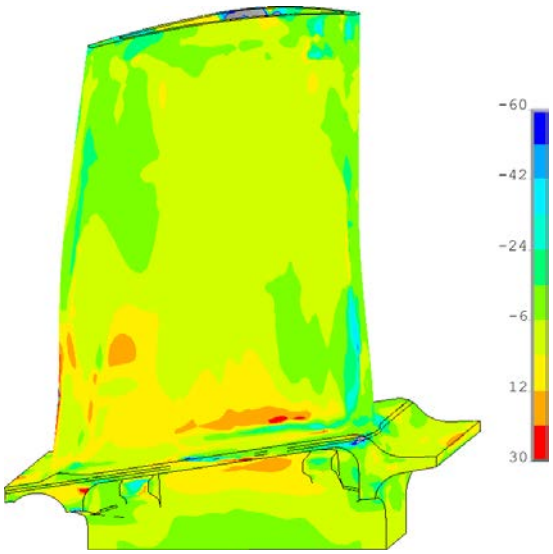

Fig. 18. Distribution of $\Delta\overline{\sigma}_{eqv}^t$,%

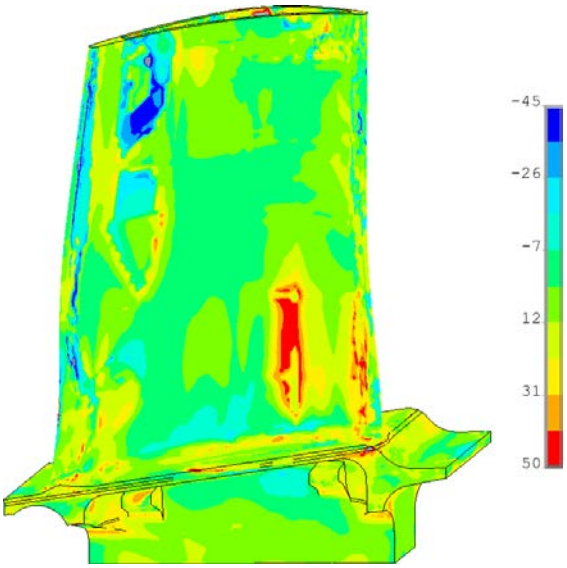

Fig. 19. Distribution of $\Delta\overline{K}_m$, %

Analysis of the results showed that when anisotropy is taken into account, the values of the estimated safety margins decreases by 20-30%. That means underestimation of the estimated life by 300-400%. It is also worth noting that the change in safety factor values is more significant than the change in stress values.

Table 2. Calculation results

Model	Zone, #	T, °C	L	σ_0, MPa	σ_{end}, MPa	σ^t_{eqv}, MPa	σ_r, MPa	K_m	Δ, %
Iso	1	1032	0.20	163	63	96	255	2.65	-
Aniso			0.19	178	71	104	288	2.76	4
Aniso*			0.10				256	2.46	-7
Iso	2	722	0.19	584	567	569	992	1.74	-
Aniso			0.20	697	628	641	813	1.27	-27
Aniso*			0.20				814	1.27	-27

*equivalent direction changing due to creep consideration

Figures 20, 21 show relaxation curve for zone #1, 2.

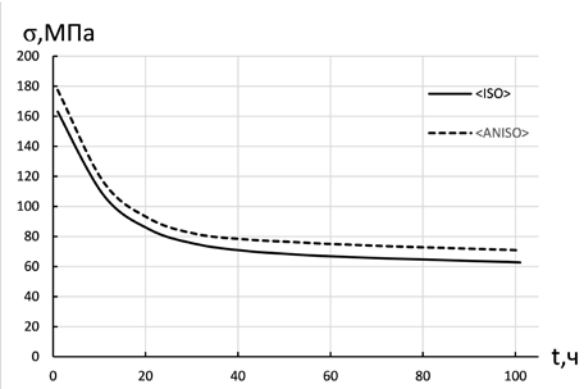

Fig. 20. Relaxation curve (zone #1)

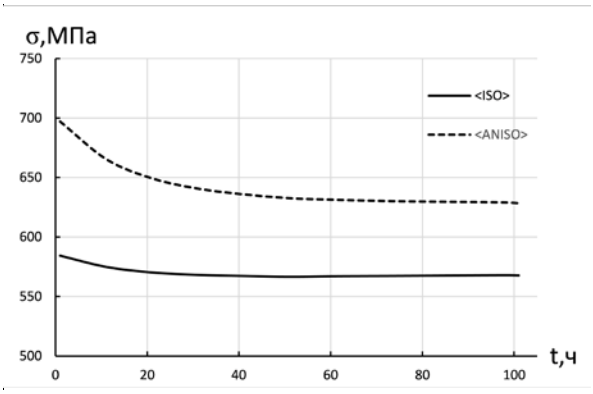

Fig. 21. Relaxation curve (zone #2)

4. Discussion

The analysis of the results showed that blade needs to be considered anisotropic. Figure 20 shows histogram of $\Delta\overline{K}_m$. For the considered blade under the given conditions and loads, it was shown that ignoring the anisotropy can lead to an underestimation of the estimated durability by 300-400%.

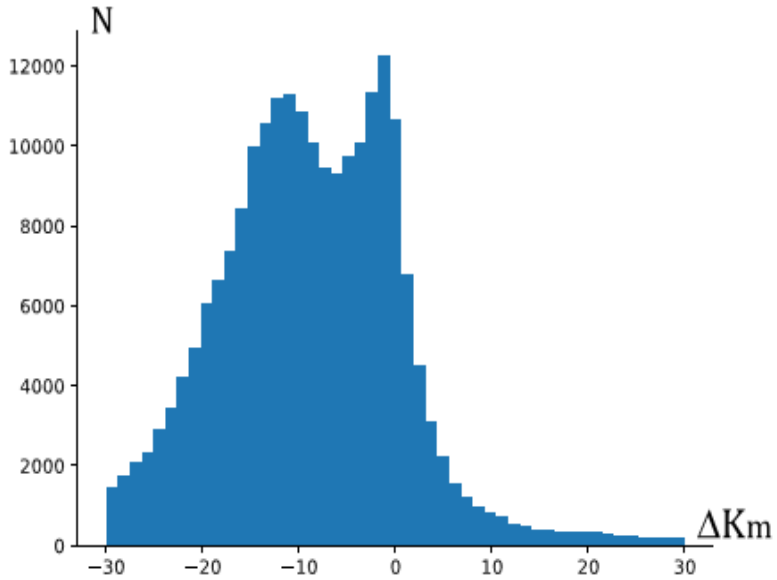

Fig. 22. Histogram of $\Delta\overline{K}_m$, %

It should be noted that this blade is characterized by a relatively simple cooling system

and a relatively simple stress state. When considering blades with a more complex cooling system, the difference in results may be even more significant. The direction of further research is the development of a method for assessing the cyclic durability of single-crystal turbine blades.

5. Conclusions

Based on the research results, the importance of taking into account the anisotropy of characteristics and the complex stress state when calculating the static strength of SX turbine blades is shown. To consider this a phenomenological model based on equivalent direction of stress state is proposed. Changing of equivalent direction due to creep should be considered.

In addition, necessity of obtaining characteristics in intermediate CO's is shown.

Acknowledgements. *Authors wishing to acknowledge assistance of colleagues that helped with experimental investigation: Mikhail Volkov, Alexander Demidov and Elena Bredikhina.*

References

[1] Vasilyev BE. Stress-Strain State Prediction of High-Temperature Turbine Single Crystal Blades Using Developed Plasticity and Creep Models. In: *Proceedings of the GT201425229 ASME Turbo Expo 2014.* American Society of Mechanical Engineers; 2014. p. V07AT29A005|-V07AT29A005.

[2] Tinga T. *Multiscale modelling of single crystal superalloys for gas turbine blades*. Eindhoven: Technische Universiteit Eindhoven; 2009.

[3] Ramaglia AD, Villari P. Creep and Fatigue of Single Crystal and Directionally Solidied Nickel-Base Blades via a Unied Approach Based on Hill48 Potential Function: Part 1 - Plasticity and Creep. In: *GT201394675 ASME Turbo Expo 2013: Turbine Technical Conference and Exposition.* American Society of Mechanical Engineers; 2013. p. V07AT27A004-V07AT27A004.

[4] Meric L, Poubanne P, Cailletaud G. Single Crystal Modeling for Structural Calculations: Part 1 – Model Presentation. *Journal of Engineering Materials and Technology*. 1991;113(1): 162-171.

[5] Meric L, Cailletaud G. Single Crystal Modeling for Structural Calculations: Part 2 – Finite Element Implementation. *Journal of Engineering Materials and Technology*. 1991;113(1): 171-182.

[6] Milligan WW, Antolovich SD. Yielding and deformation behavior of the single crystal superalloy PWA 1480. *Metallurgical Transactions.* 1987;18(1): 85-95.

[7] Allan CD. *Plasticity of Nickel-based Single Crystal Superalloy. Ph.D. thesis.* Massachusetts Institute of Technology; 1995.

[8] Raabe D, Klose P, Engl B, Imlau KP, Friedel F, Roters F. Concepts for integrating plastic anisotropy into metal forming simulations. *Advanced Engineering Materials*. 2002;4(4): 169-180.

[9] Leidermark D. *Crystal plasticity and crack initiation in a single-crystal nickel-base superalloy: Modelling, evaluation and applications. Ph.D. thesis.* Sweden: Linköping University; 2011.

[10] Semenov AS, Gestov LB, Semenov SG, Grishchenko AI. Soprotivlenie deformirovaniju i razrusheniju monokristallicheskih zharoprochnyh splavov pri staticheskom i ciklicheskom nagruzhenii. *Vestnik samarskogo gosudarstvennogo ajerokosmicheskogo universiteta imeni akademika S.P. Koroleva*. 2014;5(47): 70-79. (In Russian)

[11] Getsov LB, Semenov AS, Besschetnov VA, Grishchenko AI, Semenov SG. Long-term strength determination for cooled blades made of monocrystalline superalloys. *Thermal Engineering*. 2017;64(4): 280-287.

[12] Getsov LB, Semenov AS, Tikhomirova EA, Rybnikov AI. Thermocyclic and static-failure criteria for single-crystal superalloys of gas-turbine blades. *Materials and Technology*. 2014;48(2): 255-260.
[13] Nozhnitsky YA, Doulnev RA, Soundyrin VG. Damage mechanisms for termomechanical fatigue of aircraft engines materials. In: *Proc. AGARG Conference 569 "Thermal mechanical fatigue of aircraft engines materials"*. NATO; 1995. p.1-12.
[14] Tsuno N, Shimabayashi S, Kakehi K, Rae CMF, Reed RC. Tension/compression asymmetry in yield and creep strengths of Ni-based superalloys. In: *Proceedings of the International Symposium on Superalloys*. TMS; 2008: p.433-442.
[15] Vasilyev BE. Prediction of the kinetics of the 3D stress-strain state of high-temperature gas turbine blades with limited experimental data. In: *28th Congress of the International Council of the Aeronautical Sciences 2012*. ICAS; 2012. p.3.
[16] Simo JC, Hughes TJR. *Computational inelasticity*. New York: Springer; 1998.